

See discussions, stats, and author profiles for this publication at: <https://www.researchgate.net/publication/231171775>

Electron Transfer Kinetics at Modified Carbon Electrode Surfaces: The Role of Specific Surface Sites

ARTICLE *in* ANALYTICAL CHEMISTRY · SEPTEMBER 1995

Impact Factor: 5.64 · DOI: 10.1021/ac00114a004

CITATIONS

195

READS

27

3 AUTHORS, INCLUDING:



[Richard McCreery](#)

University of Alberta

177 PUBLICATIONS 9,464 CITATIONS

SEE PROFILE

Electron Transfer Kinetics at Modified Carbon Electrode Surfaces: The Role of Specific Surface Sites

Peihong Chen, Mark A. Fryling, and Richard L. McCreery*

Department of Chemistry, The Ohio State University, 120 West 18th Avenue, Columbus, Ohio 43210

The electron transfer (ET) kinetics of $\text{Ru}(\text{NH}_3)_6^{3+/2+}$, $\text{IrCl}_6^{2-/3-}$, $\text{Fe}(\text{CN})_6^{3-/4-}$, $\text{Fe}_{\text{aq}}^{2+/3+}$, and $\text{V}_{\text{aq}}^{2+/3+}$ were examined on several modified glassy carbon surfaces. The kinetics of the aquated ions were very sensitive to the density of surface oxides, while those of the other redox systems were not. In particular, chemical derivatization of surface carbonyl groups decreased the rate of electron transfer with $\text{Fe}^{3+/2+}$ by 2–3 orders of magnitude but had little effect on $\text{Ru}(\text{NH}_3)_6^{3+/2+}$ or $\text{IrCl}_6^{2-/3-}$. The electron transfer rates for $\text{Fe}^{3+/2+}$ correlated with surface C=O density determined by resonance Raman spectroscopy. Neutral, cationic, and anionic nonspecific adsorbers decreased the rates of ET with the aquated ions approximately equally but had little effect on $\text{Ru}(\text{NH}_3)_6^{2-/3+}$. The redox systems studied were classified into two groups: those which are catalyzed by surface carbonyl groups and those which are not. Possible catalytic mechanisms are considered.

A significant effort by many laboratories has been directed toward understanding the relationship between surface structure and electron transfer reactivity for carbon electrodes.^{1–9} Complex surface chemistry and an often unknown level of surface impurities have made it difficult to determine the important structural variables controlling carbon electrode reactivity. At least three major phenomena affect electron transfer (ET) reactivity, and these vary in importance for different redox systems and solution conditions. First, many redox systems (e.g., $\text{Fe}(\text{CN})_6^{3-/4-}$, ascorbic acid, dopamine) are very sensitive to surface cleanliness, and observed ET rates are strongly dependent on surface history.^{4,10} Second, the microstructure of the carbon has a large effect on most redox systems, with the basal plane of highly ordered pyrolytic graphite (HOPG) exhibiting much slower ET

than glassy carbon (GC).^{10–12} Third, some redox systems are sensitive to the presence of surface oxides, which act as catalysts for electron transfer^{13–15} or modify the surface charge.¹⁶ Unfortunately, many common electrode surface preparation procedures affect more than one of these three variables. For example, electrochemical pretreatment (ECP) by anodization of the surface^{7,8,17} changes the carbon microstructure, removes impurities, and forms surface oxides.¹ Thus it is difficult to determine which factor underlies the kinetic changes induced by ECP.

In several previous reports, we examined the effects of carbon microstructure,^{10–12,18} cleanliness,^{10,19} and surface oxidation^{9,20} on a variety of redox systems, mostly transition metal complexes. Several conclusions which are relevant to the present work should be summarized here. First, 17 inorganic complexes and four organic redox systems exhibit much slower ET rates on HOPG compared to GC, a shortfall we attribute to the low density of electronic states in HOPG.¹² Second, disordering of HOPG by laser activation or ECP increases ET rates for most systems to values close to those observed on clean GC. Third, $\text{Fe}_{\text{aq}}^{2+/3+}$, $\text{V}_{\text{aq}}^{2+/3+}$, and $\text{Eu}_{\text{aq}}^{2+/3+}$ are further accelerated by the presence of surface oxides to ET rates well above the outer-sphere values predicted from homogeneous self-exchange rates via Marcus theory.⁹ Fourth, this oxide catalysis is not consistent with mechanisms based on redox mediation, hydrophobic effects, or double layer effects.

Combined with the extensive literature on electrochemistry at carbon, these observations lead to a working hypothesis on the structural basis of ET reactivity at carbon.^{1,21} Outer-sphere systems such as $\text{Ru}(\text{NH}_3)_6^{2+/3+}$, $\text{IrCl}_6^{2-/3-}$, etc. are sensitive to the electronic structure of the carbon (due to the electronic density of states, DOS) but are otherwise insensitive to surface functional groups or impurities. The effect of low DOS is nonspecific and applies to all 21 redox systems examined to date. In addition,

- (1) McCreery, R. L. In *Electroanalytical Chemistry*; Bard, A. J., Ed.; Dekker: New York, 1991; Vol. 17, pp 221–374.
- (2) Kinoshita, K. *Carbon: Electrochemical and Physicochemical Properties*; Wiley: New York, 1988.
- (3) Sarangapani, S.; Akridge, J. R.; Schumm, B., Eds. *Proceedings of the Workshop on the Electrochemistry of Carbon*; The Electrochemical Society: Pennington, NJ, 1984.
- (4) Hu, I. F.; Kuwana, T. *Anal. Chem.* **1986**, *58*, 3235.
- (5) Wightman, R. M.; Deakin, M. R.; Kovach, P. M.; Kuhr, W. G.; Stutts, K. J. *J. Electrochem. Soc.* **1984**, *131*, 1578.
- (6) Hu, I. F.; Karweik, D. H.; Kuwana, T. *J. Electroanal. Chem.* **1985**, *188*, 59.
- (7) Engstrom, R. C.; Strasser, V. A. *Anal. Chem.* **1984**, *56*, 136.
- (8) Cabaniss, G. E.; Diamantis, A. A.; Murphy, W. R., Jr.; Linton, R. W.; Meyer, T. J. *J. Am. Chem. Soc.* **1985**, *107*, 1845.
- (9) McDermott, C. A.; Kneten, K. R.; McCreery, R. L. *J. Electrochem. Soc.* **1993**, *140*, 2593.

- (10) Rice, R. J.; Pontikos, N. M.; McCreery, R. L. *J. Am. Chem. Soc.* **1990**, *112*, 4617.
- (11) Kneten, K. R.; McCreery, R. L. *Anal. Chem.* **1992**, *64*, 2518.
- (12) Cline, K. K.; McDermott, M. T.; McCreery, R. L. *J. Phys. Chem.* **1994**, *98*, 5314.
- (13) Evans, J. F.; Kuwana, T. *Anal. Chem.* **1977**, *49*, 1632.
- (14) Tse, D. C. S.; Kuwana, T. *Anal. Chem.* **1978**, *50*, 1315.
- (15) Armstrong, F. A.; Bond, A. M.; Hill, H. A. O.; Olive, B. N.; Psalti, I. S. M. *J. Am. Chem. Soc.* **1989**, *111*, 9185.
- (16) Deakin, M. R.; Stutts, K. J.; Wightman, R. M. *J. Electroanal. Chem.* **1985**, *182*, 113.
- (17) Barbero, C.; Silber, J. J.; Sereno, L. J. *Electroanal. Chem.* **1988**, *248*, 321.
- (18) Rice, R. J.; McCreery, R. L. *Anal. Chem.* **1989**, *61*, 1637.
- (19) Poon, M.; McCreery, R. L.; Engstrom, R. *Anal. Chem.* **1988**, *60*, 1725.
- (20) Allred, C. D.; McCreery, R. L. *Anal. Chem.* **1992**, *64*, 444.
- (21) McCreery, R. L.; Cline, K. K.; McDermott, C. A.; McDermott, M. T. *Colloids Surf. A* **1994**, *93*, 211.

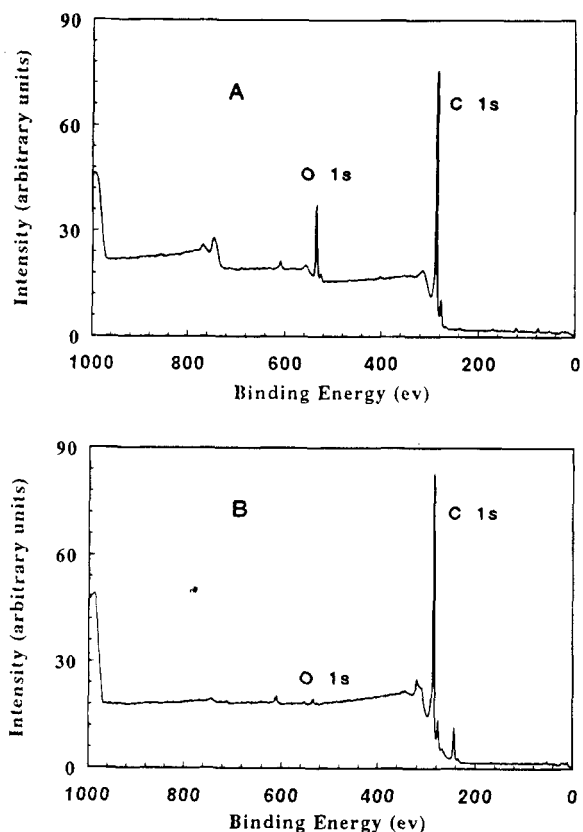


Figure 1. XPS survey spectra of (A) polished GC and (B) argon-sputtered GC.

there are many redox reactions, such as that of $\text{Fe}_{\text{aq}}^{2+/3+}$, which are catalyzed by specific interactions with surface oxides⁹ and are therefore very sensitive to surface chemistry. The current experiments were designed to test this hypothesis in detail for several representative redox systems, including $\text{Ru}(\text{NH}_3)_6^{2+/3+}$ and $\text{Fe}_{\text{aq}}^{2+/3+}$. Various preparation techniques were used to vary the nature and density of surface functional groups before observing ET reactivity. By combining independent measures of oxide functional groups based on Raman spectroscopy and XPS with observations of kinetic behavior, the relationship between surface structure and ET rate was revealed.

EXPERIMENTAL SECTION

In all cases except in the study of argon-sputtered GC electrodes, the GC electrodes used were from Bioanalytical Systems Inc. (MF2070). In the case of argon sputtering pretreatment, Tokai GC-20 plates from Applied Industrial Material Co. were used. Polished GC electrodes were prepared by initial sanding with SiC paper when necessary and then polishing with successive slurries of 1, 0.3, and 0.05 μm alumina (Buehler) in Nanopure water on Microcloth polishing cloth (Buehler). Polished GC electrodes were sonicated in Nanopure water (Barnstead) for about 10 min before being placed into the electrochemical cell or further treatment. During transfers between each step, the surfaces of GC electrodes were kept wet to reduce contamination from air.

Argon sputtering treatment was carried out in the vacuum chamber of an XPS/Auger spectrometer (VG Scientific). The vacuum chamber was pumped to 10^{-9} Torr, then filled with argon gas to a pressure of 2×10^{-6} Torr. The GC surface was sputtered with an AG21 argon source (VG Scientific) at a focus energy of

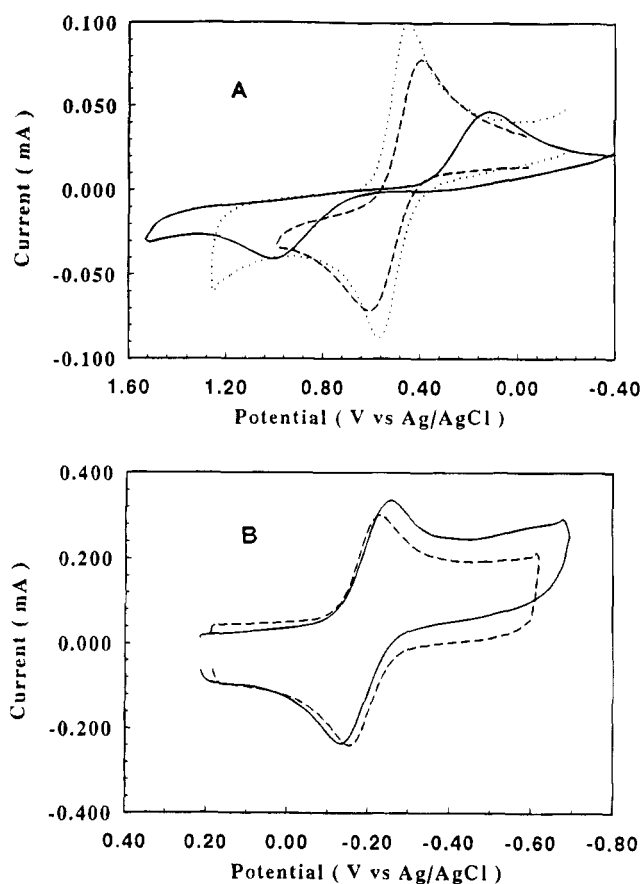


Figure 2. Voltammograms of (A) 5 mM $\text{Fe}^{3+/2+}$ in 0.2 M HClO_4 at polished (dashed line), argon-sputtered (solid line), and argon-sputtered/ECP (dotted line) GC electrodes (scan rate, 0.2 V/s; ECP procedure was seven cycles from 0 to 2.2 V in 1.2 M H_2SO_4 at 0.2 V/s) and (B) 1 mM $\text{Ru}(\text{NH}_3)_6^{3+/2+}$ in 1 M KCl at polished (dashed line) and argon-sputtered (solid line) GC electrodes (scan rate, 20 V/s).

3.6 kV and target current of 30 μA for 10 min. XPS survey spectra were obtained before and after argon sputtering with a VG Scientific XPS spectrometer (Mg X-ray radiation source). The GC pieces were transferred into 0.2 M HClO_4 solution immediately after they were taken from the vacuum system, and electrochemical measurements were carried out within 5 min.

2,4-DNPH derivatization of GC electrode surfaces and Raman measurement of the derivatized surfaces were performed as described previously.²² Preceding electrochemical experiments on derivatized electrodes, the electrodes were rinsed thoroughly in 20 mL of Nanopure water twice before transfer into the electrochemical cell. To derivatize the electrode surface with 3,5-dinitrobenzoyl chloride, the electrode was polished and rinsed with pyridine, immersed in 0.1 M 3,5-dinitrobenzoyl chloride/pyridine solution, and heated on a hot plate for 1 min. After standing in the solution for 1 h, the electrode was thoroughly rinsed with pyridine followed by Nanopure water.

2,6-Anthraquinone disulfonate (AQDS) was adsorbed to GC electrodes by placing polished GC electrodes in 10 mM 2,6-AQDS aqueous solution for 10 min and rinsing in 30 mL of Nanopure water successively three times. The electrodes were then transferred into an electrochemical cell containing 0.1 M HClO_4 for voltammetry.

Methylene blue (MB) was adsorbed on GC electrodes by dipping polished GC in 0.1 mM MB in water for 10 min and rinsing

(22) Fryling, M. A.; Zhao, J.; McCreery, R. L. *Anal. Chem.* **1995**, 67, 967.

Table 1. Electron Transfer Rate Constants (in cm/s) of Some Inner-Sphere and Outer-Sphere Redox Systems at Modified GC Electrode

	polished GC	argon-sputtered GC	DNPH-treated GC	dinitrobenzoyl chloride-treated GC	2,6-AQDS-adsorbed GC	methylene blue-adsorbed GC	BMB-adsorbed GC
$\text{Ru}(\text{NH}_3)_6^{3+/2+}$	0.24 ± 0.07^a	0.039 ± 0.005	0.13 ± 0.01	0.15 ± 0.08	0.15 ± 0.02	$>0.093 \pm 0.005$	0.13 ± 0.02
$\text{IrCl}_6^{3-/4-}$	0.50 ± 0.06	0.11 ± 0.13	0.21 ± 0.04		0.25 ± 0.05	0.22 ± 0.03	0.20 ± 0.04
$\text{Fe}(\text{CN})_6^{3-/4-}$	0.10 ± 0.02	0.037 ± 0.009	0.026 ± 0.006	0.084 ± 0.030	0.047 ± 0.008	0.078 ± 0.005	0.076 ± 0.004
$\text{Fe}_{\text{aq}}^{2+/3+}$	$(2.5 \pm 0.3) \times 10^{-3}$	$(2.1 \pm 1.3) \times 10^{-6}$	$(1.6 \pm 1.2) \times 10^{-5}$	$(1.1 \pm 0.5) \times 10^{-3}$	$(7.4 \pm 2.8) \times 10^{-3}$	$(3.8 \pm 0.3) \times 10^{-4}$	$(9.1 \pm 3.0) \times 10^{-5}$
$\text{Eu}_{\text{aq}}^{2-/3+}$	$(8.4 \pm 1.4) \times 10^{-4}$		$<6.0 \times 10^{-6}$				
$\text{V}_{\text{aq}}^{2+/3+}$	$(6.8 \pm 4.0) \times 10^{-4}$	$<2.0 \times 10^{-5}$	$<1.0 \times 10^{-6}$	$(7.8 \pm 2.4) \times 10^{-5}$	$(2.1 \pm 1.0) \times 10^{-3}$	$(2.9 \pm 1.3) \times 10^{-6}$	$<1.5 \times 10^{-6}$

^a Standard derivatization, $N = 3$.

with 30 mL of Nanopure water three times. Raman spectra of MB were obtained with a spectrometer based on a single-stage spectrograph (Instruments SA, HR 640) with a 300/mm (1.0 μm blaze) grating coupled to a CCD (Photometric CH260 camera head/EEV 05-10 CCD with 296×1152 pixels, $0.66 \text{ cm} \times 2.59 \text{ cm}$ active area).²³ Excitation was provided by a tunable Ti:sapphire laser (Coherent Model 890) operating at 691 nm, pumped by a 5 W argon ion laser (Coherent Model 90).

To adsorb 1,4-bis(2-methylstyryl)benzene (BMB) on GC electrodes, polished GC was first immersed in 1 mM BMB in acetone for 10 min and then rinsed twice with 10 mL of acetone, followed by two rinses with 30 mL of Nanopure water.

The redox systems studied were as follows: 1 and 5 mM Fe^{2+} in 0.2 M HClO_4 solutions made from $\text{FeNH}_4(\text{SO}_4)_2 \cdot 12\text{H}_2\text{O}$ (Mallinckrodt, Inc.) and 70% HClO_4 (GFS Chemicals); 3 mM V^{3+} in 0.2 M HClO_4 solution made from VCl_3 (Aldrich Chemical Co.); 5 mM Eu^{3+} in 0.2 M HClO_4 solution made from $\text{Eu}(\text{NO}_3)_3 \cdot 5\text{H}_2\text{O}$ (Aldrich); 1 mM $\text{Ru}(\text{NH}_3)_6^{3+}$ in 1 M KCl solution made from $\text{Ru}(\text{NH}_3)_6\text{Cl}_3$ (Strem Chemicals); 0.5 mM IrCl_6^{2-} in 1 M KCl solution made from K_2IrCl_6 (Aldrich); 2 mM $\text{Co}(\text{en})_3^{3+}$ in 1 M KCl solution made from $\text{Co}(\text{en})_3\text{Cl}_3$ (J. T. Baker); $\text{Fe}(\text{CN})_6^{3-/4-}$ in 1 M KCl made from $\text{K}_4\text{Fe}(\text{CN})_6$ (J. T. Baker).

Other solutions included 10 mM 2,6-AQDS solution (Aldrich, recrystallized from water after being filtered through activated charcoal);²⁴ 0.1 mM methylene blue (Aldrich); 10 mM 2,4-DNPH (J. T. Baker) with 1% HCl (J. T. Baker) in dry ethanol (Quantum Chemical); 0.1% KOH (Jenneile Enterprises) in dry ethanol, 0.1 M 3,5-dinitrobenzoyl chloride (Aldrich) in pyridine (Mallinckrodt), and 1 M H_2SO_4 (Mallinckrodt). All solutions were prepared daily with distilled Nanopure water unless noted otherwise.

Cyclic voltammetry was performed with a computer triggered function generator (Tektronix) and Labmaster A/D converter. A Bioanalytical Systems Ag/AgCl (3 M NaCl) reference electrode and a platinum counter electrode were used. Electron transfer rate constants (k° , cm s^{-1}) were determined from voltammetric data using the commercial simulation program Digisim (Bioanalytical Systems). k° for the simulation was varied to match the ΔE_p values for experimental and simulated voltammograms. Although the value of the transfer coefficient (α) does not greatly affect ΔE_p , it was assumed to equal 0.5.

RESULTS

Several different manipulations of surface oxide density were carried out, and then the surface was characterized with XPS or

Raman spectroscopy before kinetic evaluation with $\text{Ru}(\text{NH}_3)_6^{2+/3+}$, $\text{Fe}_{\text{aq}}^{2+/3+}$, $\text{V}_{\text{aq}}^{2+/3+}$, $\text{Fe}(\text{CN})_6^{3-/4-}$, etc. Surface manipulations are separated into three groups: nonspecific removal of surface oxides by Ar^+ ion sputtering, chemical derivatization of specific surface oxides, and nonspecific adsorption of surface monolayers.

Ar^+ Sputtering. XPS survey spectra of polished GC-20 before and after Ar^+ sputtering in UHV are shown in Figure 1. Sputtering reduces the observed surface O/C ratio from 14% to less than 1%. After the GC specimen was quickly transferred (through air) to an electrochemical cell, the voltammograms of Figure 2 were obtained. Sputtering causes a 3 order of magnitude decrease in the ET rate for $\text{Fe}_{\text{aq}}^{2+/3+}$, while it has a relatively small effect (a factor of 6) on $\text{Ru}(\text{NH}_3)_6^{2+/3+}$. Electrochemical oxidation of the sputtered surface restores the observed $\text{Fe}_{\text{aq}}^{2+/3+}$ rate to a value somewhat higher than that on a polished surface. The observed rate constants are listed in Table 1, along with those for $\text{IrCl}_6^{2-/3-}$, $\text{V}_{\text{aq}}^{2-/3+}$, and $\text{Fe}(\text{CN})_6^{3-/4-}$ following similar treatments. These results reveal that Ar^+ sputtering decreases the rate constants of $\text{Fe}_{\text{aq}}^{2+/3+}$ and $\text{V}_{\text{aq}}^{2+/3+}$ by a much larger factor than those of $\text{IrCl}_6^{2-/3-}$, $\text{Ru}(\text{NH}_3)_6^{2+/3+}$, or $\text{Fe}(\text{CN})_6^{3-/4-}$. As is apparent from Figure 2A and several reports in the literature, electrochemical oxidation of GC dramatically increases k° for $\text{Fe}_{\text{aq}}^{2+/3+}$, $\text{V}_{\text{aq}}^{2+/3+}$, and $\text{Eu}_{\text{aq}}^{2+/3+}$. After ECP conditions similar to those used here, we observed k° values of 0.012, 0.009 and 0.004 cm/sec, for $\text{Fe}_{\text{aq}}^{2+/3+}$, $\text{V}_{\text{aq}}^{2+/3+}$ and $\text{Eu}_{\text{aq}}^{2+/3+}$, respectively.⁹

Specific Surface Derivatization. To examine the role of specific oxygen-containing functional groups on electrode kinetics, GC surfaces were treated with two organic reagents. Dinitrophenylhydrazine (DNPH) has been shown to specifically derivatize surface carbonyl groups, but not lactones, carboxylates, or alcohol groups.²² DNPH forms a resonance Raman active adduct which may be observed quantitatively at 1–10% surface coverage by monitoring the peak area of the 1140 cm^{-1} N–N stretch. The voltammograms of Figure 3 and the fourth column of Table 1 indicate that DNPH treatment of a polished GC surface decreases the rates of $\text{Ru}(\text{NH}_3)_6^{3+/2+}$ and $\text{IrCl}_6^{2-/3-}$ by about 50%. However, the rates of $\text{Fe}_{\text{aq}}^{2+/3+}$, $\text{Eu}_{\text{aq}}^{2+/3+}$, and $\text{V}_{\text{aq}}^{2+/3+}$ decreased by factors of more than 100 following DNPH derivatization. We noted during control experiments that ethanol decreased the $\text{Fe}_{\text{aq}}^{2+/3+}$ rate by about a factor of 10 without DNPH treatment. The experiment was repeated with a DNPH reagent in 2 M HCl without ethanol. The rate following DNPH treatment with ethanol absent was 3.6×10^{-5} , while a control experiment with 2 M HCl yielded $k^\circ = 1.8 \times 10^{-3}$. The 2M HCl treatment had no effect on the $\text{Ru}(\text{NH}_3)_6^{2+/3+}$ rate constant. Thus DNPH treatment consistently reduced the $\text{Fe}_{\text{aq}}^{2+/3+}$ by a factor of 70–100 whether or not ethanol was present,

(23) Frank, C. J.; Redd, D. C. B.; Gansler, T. S.; McCreery, R. L. *Anal. Chem.* **1994**, *66*, 319.

(24) He, P.; Crooks, R. M.; Faulkner, L. R. *J. Phys. Chem.* **1990**, *94*, 1135.

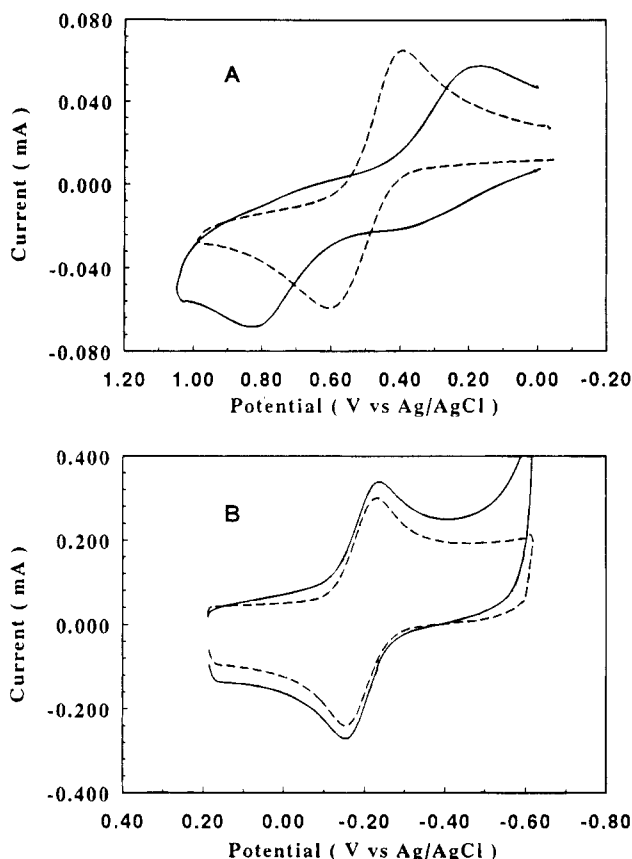


Figure 3. Voltammograms of (A) 5 mM $\text{Fe}^{3+/2+}$ in 0.2 M HClO_4 at polished (dashed line) and DNPH-treated (solid line) GC electrodes ($\nu = 0.2$ V/s) and (B) 1 mM $\text{Ru}(\text{NH}_3)_6^{3+/2+}$ in 1 M KCl at polished (dashed line) and DNPH-treated (solid line) GC electrodes (ν V/s).

Table 2. Correlation between Raman Detected Carbonyl Density and the Electron Transfer Rate Constant of $\text{Fe}_{\text{aq}}^{2+/3+}$

surface treatment	area under DNPH-carbon adduct 1140 cm^{-1} Raman band (e^-)	electron transfer rate for $\text{Fe}_{\text{aq}}^{2+/3+}$ ($\text{cm/s})^a$
polished	270 ± 32^b	2.5×10^{-3}
ECP 10 s, 2.2 V, 1 M NaOH	274 ± 63	2.0×10^{-3}
ECP 10 s, 1.5 V, 1.5 M H_2SO_4	525 ± 52	3.6×10^{-3}
ECP 10 s, 2.2 V, 1 M, HNO_3	575 ± 154	3.2×10^{-3}
ECP 10 s, 2.2 V, 1 M, NaNO_3	848 ± 174	3.6×10^{-3}
ECP 5 s, 1.8 V, 1 M H_2SO_4	1716 ± 351	7.1×10^{-3}
ECP 10 s, 2.2 V, 1 M H_2SO_4	3175 ± 416	1.0×10^{-2}

^a Standard derivatization, $N \geq 3$. ^b Before DNPH derivatization. Two identical samples were electrochemically pretreated, and then one was used for $\text{Fe}^{2+/3+}$ voltammetry, the other for DNPH derivatization and Raman spectroscopy.

while neither DNPH nor ethanol affected the $\text{Ru}(\text{NH}_3)_6^{2+/3+}$ rate significantly.

In a previous report, we demonstrated that surface carbonyl density could be determined from the area of the 1140 cm^{-1} band of the resonance-enhanced, surface-bound DNPH.²² The relationship between k^0 for $\text{Fe}_{\text{aq}}^{2+/3+}$ and DNPH coverage is shown in Table 2 and Figure 4. The carbonyl density was increased by ECP under various conditions (shown in Table 2), and then $\text{Fe}_{\text{aq}}^{2+/3+}$ voltammograms were obtained. An identically treated surface was subjected to DNPH derivatization, and then Raman spectra were obtained to evaluate $\text{C}=\text{O}$ coverage. The 1140 cm^{-1} peak area indicates the density of surface $\text{C}=\text{O}$ groups, with an

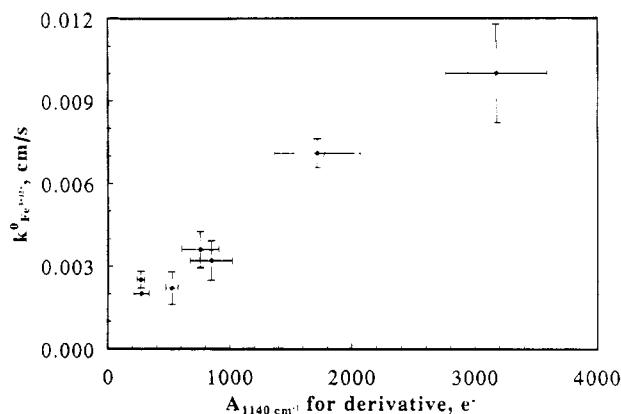


Figure 4. Correlation between the area of 1140 cm^{-1} DNPH-carbon adduct Raman band and rate constant of $\text{Fe}^{3+/2+}$ at carbon electrodes after ECP with various procedures. The ECP procedures are listed in Table 2. Rate constants were determined *before* DNPH derivatization. The 1140 cm^{-1} Raman band was observed *after* DNPH derivatization and indicates the surface carbonyl density.

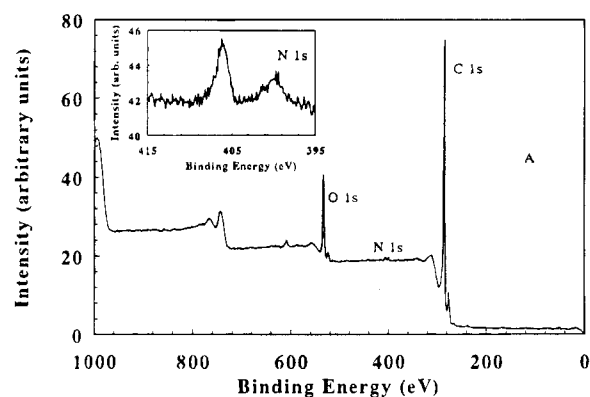


Figure 5. (A) XPS survey spectrum of DNBC-treated GC surface. Inset shows magnified nitrogen 1s region. (B) Voltammograms of 5 mM $\text{Fe}^{3+/2+}$ in 0.2 M HClO_4 on polished (dashed line) and DNBC-treated (solid line) GC electrodes ($\nu = 0.2$ V/s). (C) Voltammograms of 1 mM $\text{Ru}(\text{NH}_3)_6^{3+/2+}$ in 1 M KCl on polished (dashed line) and DNBC-treated (solid line) GC electrodes ($\nu = 20$ V/s).

area of 270 e^- corresponding to $\sim 1\%$ of a monolayer. As the surface $\text{C}=\text{O}$ increases, k^0 for $\text{Fe}_{\text{aq}}^{2+/3+}$ also increases, monotonically and roughly linearly. The results establish a direct correlation between $\text{Fe}_{\text{aq}}^{2+/3+}$ ET rate and surface carbonyl density.

Although it was not studied in as much detail, dinitrobenzoyl chloride (DNBC) is a reagent which should react with surface OH groups to form a dinitrophenyl ester.²⁵ After reaction with DNBC, polished GC exhibited a nitrogen 1s peak from the surface-bound NO_2 group, with a surface coverage of $\sim 1\%$ (Figure 5). Voltammetry showed minor effects of DNBC on $\text{Fe}_{\text{aq}}^{2+/3+}$ and $\text{Ru}(\text{NH}_3)_6^{3+/2+}$ ET rates. The kinetic effects of DNBC derivatization are summarized in Table 1 for four redox systems.

(25) Siggia, S.; Hanna, J. G. *Quantitative Organic Analysis via Functional Group*; Wiley: New York, 1979; pp 31–40, 61–71.

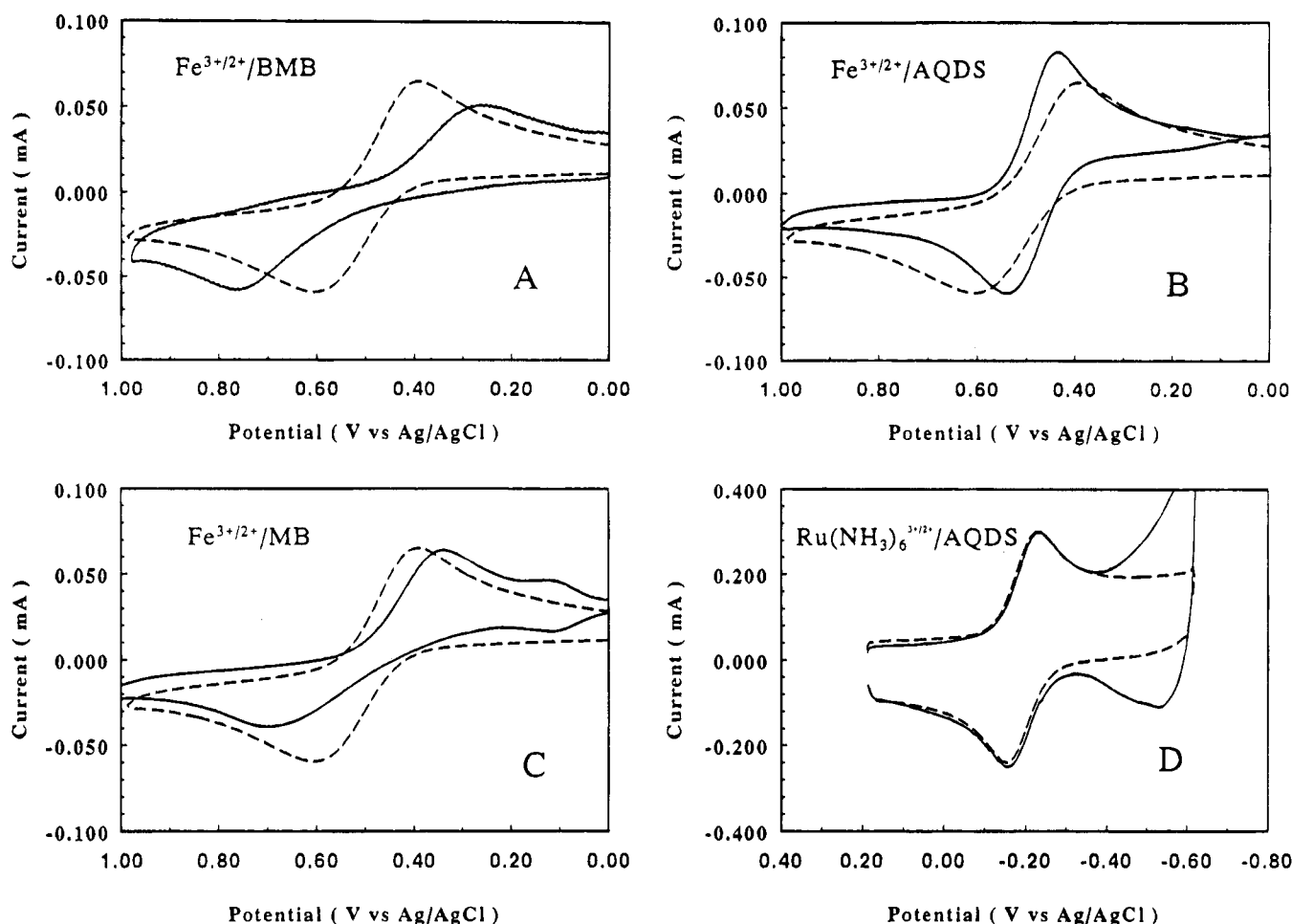


Figure 6. Voltammograms of (A) 5 mM $\text{Fe}^{3+/2+}$ in 0.2 M HClO_4 at polished (dashed line) and BMB treated (solid line) GC electrodes ($\nu = 0.2$ V/s); (B) 5 mM $\text{Fe}^{3+/2+}$ in 0.2 M HClO_4 at polished (dashed line) and AQDS-treated (solid line) GC electrodes ($\nu = 0.2$ V/s); (C) 5 mM $\text{Fe}^{3+/2+}$ in 0.2 M HClO_4 at polished (dashed line) and methylene blue-treated (solid line) GC electrodes ($\nu = 0.2$ V/s); and (D) 1 mM $\text{Ru}(\text{NH}_3)_6^{3+/2+}$ in 1 M KCl at polished (dashed line) and AQDS-treated (solid line) GC electrodes ($\nu = 20$ V/s). Conditions for adsorption of BMB, AQDS, and MB are indicated in the text.

Nonspecific Adsorption. The surface coverage of DNPH and DNBC on polished GC is on the order of the original oxide coverage, a few percent. We have demonstrated previously that anthraquinone 2,6-disulfonate (AQDS) and bis(4-methylstyryl)-benzene (BMB) physisorb on GC at monolayer levels.^{26,27} AQDS forms a monolayer when adsorbed from dilute aqueous solution and can be detected voltammetrically. BMB forms a monolayer from acetone solution and is observable with Raman spectroscopy.²⁸ Figure 6 shows that methylene blue (MB) adsorbs strongly to polished GC from 0.1 mM aqueous solution, with the voltammogram of Figure 6A indicating a surface coverage of 190 pmol/cm². Resonance Raman spectra of adsorbed MB before (Figure 6B) and after (Figure 6C) voltammetry in $\text{Fe}_{\text{aq}}^{2+/3+}$ solution indicate that the MB is strongly adsorbed and does not desorb during voltammetry in a solution which does not contain MB.

The kinetic effects of these nonspecific adsorbers on $\text{Fe}_{\text{aq}}^{2+/3+}$ and $\text{Ru}(\text{NH}_3)_6^{3+/2+}$ are shown in Figure 7, and Table 1. BMB and MB have small negative effects on $\text{Ru}(\text{NH}_3)_6^{3+/2+}$ and $\text{IrCl}_6^{2-/3-}$ rate constants but decrease the $\text{Fe}_{\text{aq}}^{2+/3+}$ and $V_{\text{aq}}^{2+/3+}$ rates by

about an order of magnitude. AQDS adsorption also decreases the $\text{Ru}(\text{NH}_3)_6^{2+/3+}$ and $\text{IrCl}_6^{2-/3-}$ rate constants slightly but increases the $\text{Fe}_{\text{aq}}^{2+/3+}$ and $V_{\text{aq}}^{2+/3+}$ rates.

Finally, adsorption of $\text{Fe}^{2+/3+}$ and $\text{Ru}(\text{NH}_3)_6^{3+/2+}$ was examined using the semiintegral approach described elsewhere.²⁹ The semiintegral of a $\text{Ru}(\text{NH}_3)_6^{3+/2+}$ voltammogram (Figure 8A) exhibits the ideal sigmoidal shape expected for a diffusion-controlled process. After ECP, a similar sigmoidal semiintegral was observed, with a slight peak on the plateau indicating weak adsorption of $\text{Ru}(\text{NH}_3)_6^{3+/2+}$ to the oxidized surface (Figure 8B). The semiintegral for the oxidation of $\text{Fe}_{\text{aq}}^{2+}$ on a polished GC surface (Figure 8C) clearly indicates adsorption, which is increased significantly by ECP (Figure 8D). A rough estimate of the amount of adsorbed Fe^{2+} for the polished surface shown in Figure 8C yields ~ 40 pmol/cm².

DISCUSSION

The redox systems in Table 1 fall into two distinct groups, which differ in their sensitivity to surface chemistry. $\text{Ru}(\text{NH}_3)_6^{3+/2+}$, $\text{IrCl}_6^{2-/3-}$, and $\text{Fe}(\text{CN})_6^{3-/4-}$ exhibit relatively small decreases in k° upon Ar^+ sputtering, derivatization of surface C=O or C-OH, and nonspecific adsorption. It is somewhat surprising that a

(26) McDermott, M. T.; Kneten, K.; McCreery, R. L. *J. Phys. Chem.* **1992**, *96*, 3124.

(27) McDermott, M. T.; McCreery, R. L. *Langmuir*, in press.

(28) Kagan, M. R.; McCreery, R. L., submitted for publication.

(29) Bowling, R.; McCreery, R. L. *Anal. Chem.* **1988**, *60*, 605.

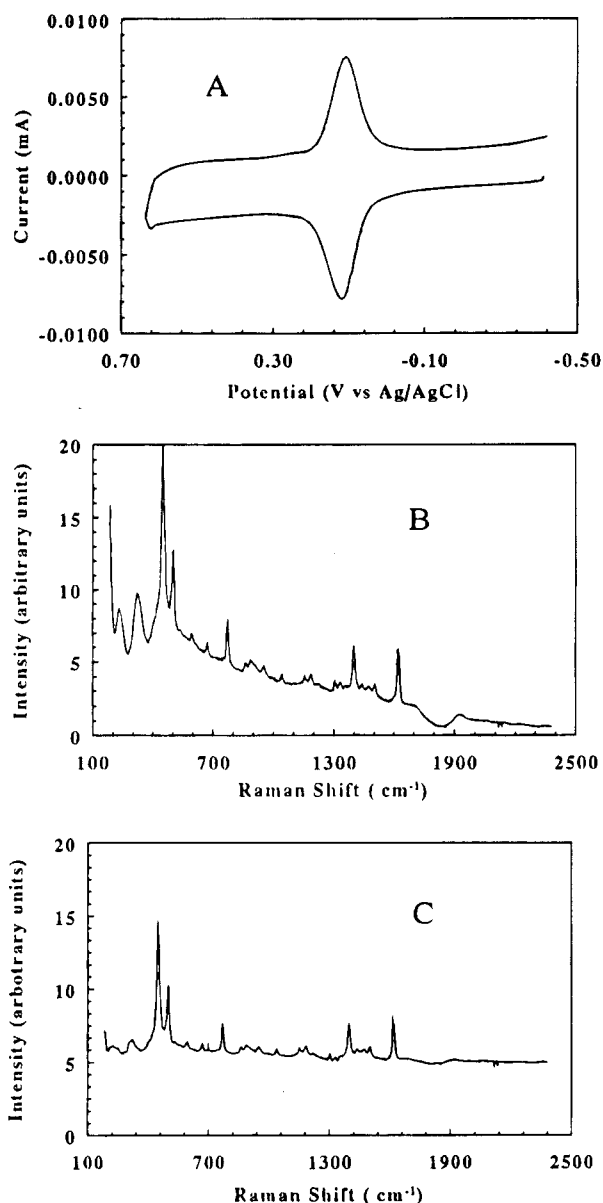


Figure 7. (A) Voltammogram of adsorbed methylene blue on GC obtained in 0.2 M HClO₄ after the electrode is immersed in 0.1 mM methylene blue solution for 10 min and washed three times in 30 mL of Nanopure water. (B) Raman spectrum of methylene blue-treated GC surface. (C) Raman spectrum of methylene blue-treated GC surface after six Fe³⁺/2⁺ voltammograms had been acquired on the same surface.

monolayer of an organic adsorbate such as BMB or AQDS decreases the rate for these systems by factors of only about 2–5. The decrease is independent of the charge of the adsorbate (–2, 0, or +2), which rules out a major contribution from double layer effects.¹⁶ It is probably an oversimplification to attribute the change solely to the increase in electron tunneling distance, but such an explanation is quantitatively reasonable. For a tunneling constant of about 1.0 Å^{–1}, a monolayer spacer between the electrode and the redox system would decrease the rate by less than an order of magnitude.³⁰

Ar⁺ sputtering should not deposit a monolayer of adsorbate (ignoring possible contamination during UHV to solution transfer) and should not inhibit ET. However, Raman spectroscopy reveals

that Ar⁺ sputtering disorders GC, with an undetermined effect on ET rates. We can conclude from the Ar⁺ sputtering treatment that reduction of surface oxide level and disordering reduce observed rates for Ru(NH₃)₆^{3+/2+} and IrCl₆^{2–/3–} by less than an order of magnitude. While Fe(CN)₆^{3–/4–} behaves similarly, previous reports for both carbon and metallic surfaces indicate that the Fe(CN)₆^{3–/4–} often behaves anomalously and should not be considered outer-sphere.^{1,12,31} Therefore, we conclude that IrCl₆^{2–/3–} and Ru(NH₃)₆^{3+/2+} are behaving as outer-sphere systems, and Fe(CN)₆^{3–/4–} will be set aside for now. Consistent with this conclusion is the observation that specific surface groups have small effects on Ru(NH₃)₆^{3+/2+} or IrCl₆^{2–/3–}, at least for the conditions employed.

The aquated metal complexes Fe_{aq}^{2+/3+}, V_{aq}^{2+/3+}, and Eu_{aq}^{2+/3+} behave much differently, exhibiting extreme sensitivity to surface chemistry. First, derivatization of carbonyl sites with DNPH decreases the rate for these systems by at least a factor of 100, even though the DNPH surface coverage is only ~1%. When DNPH was used to quantify C=O coverage rather than to block carbonyl groups, Fe_{aq}^{2+/3+} rates tracked C=O density (Figure 4). Nonspecific adsorption of MB or BMB decreased the Fe_{aq}^{2+/3+}, V_{aq}^{2+/3+}, and Eu_{aq}^{2+/3+} rates more than that of the outer-sphere systems, but not as much as DNPH. In addition, an OH specific reagent had a fairly small effect on Fe_{aq}^{3+/2+} and V_{aq}^{2+/3+}. Collectively, these observations indicate the central role of surface C=O groups in accelerated ET to the aquated systems studied.

Unlike BMB and MB, AQDS adsorption *increases* the rate constants for Fe_{aq}^{3+/2+} and V_{aq}^{2+/3+}. A similar increase was observed for 1,5-AQDS and for anthraquinone monosulfate. Fe_{aq}^{2+/3+} and V_{aq}^{2+/3+} have very different formal potentials in 1 M HClO₄ (+0.5 vs –0.4 vs SCE), so catalysis by anthraquinone is unlikely to involve redox mediation. Since the anthraquinones contain C=O groups, it is possible that they increase the Fe_{aq}^{2+/3+} rate by increasing the “surface” C=O density. As an aside, it was observed that Fe_{aq}^{2+/3+} catalysis occurred when the AQDS was adsorbed from a concentrated (10 mM) solution rather than a dilute solution (10^{–5} M), implying that catalysis is favored by the edge rather than flat orientation for the adsorbed AQDS. For the edge orientation, the carbonyl groups should be more accessible to the Fe_{aq}^{2+/3+}.

The correlation between surface carbonyl density and *k*^o for the aquated systems is quite strong. At the limit of very low C=O coverages exhibited for the Ar⁺-sputtered and the DNPH-treated surface, the rate for Fe_{aq}^{2+/3+} is between 2 × 10^{–6} and 2 × 10^{–5} cm/s. This value is close to the outer-sphere rate observed on Pt and Au surfaces in the absence of chloride catalysis.³² As noted previously, it is also less than the outer-sphere rates predicted from the homogeneous self-exchange rate by about an order of magnitude.⁹ We proposed in a previous publication that surface oxides provided an inner-sphere route for Fe_{aq}^{2+/3+}, Eu_{aq}^{2+/3+}, and V_{aq}^{3+/2+}, possibly involving a surface C=O and an adjacent OH group.⁹ Based on this hypothesis, the nonspecific adsorbates BMB and MB decrease the Fe_{aq}^{2+/3+} rate by blocking C=O sites but apparently not as effectively as covalent bonding to DNPH. In addition, ECP increases the C=O density, thereby increasing inner-sphere catalysis for these systems.

(31) Peter, L. M.; Durr, W.; Bindra, P.; Gerischer, H. *J. Electroanal. Chem.* **1976**, *71*, 31.

(32) Hung, N. C.; Nagy, Z. *J. Electrochem. Soc.* **1987**, *134*, 2215.

(30) Finklea, H. O.; Hanshaw, D. D. *J. Am. Chem. Soc.* **1992**, *114*, 3173.

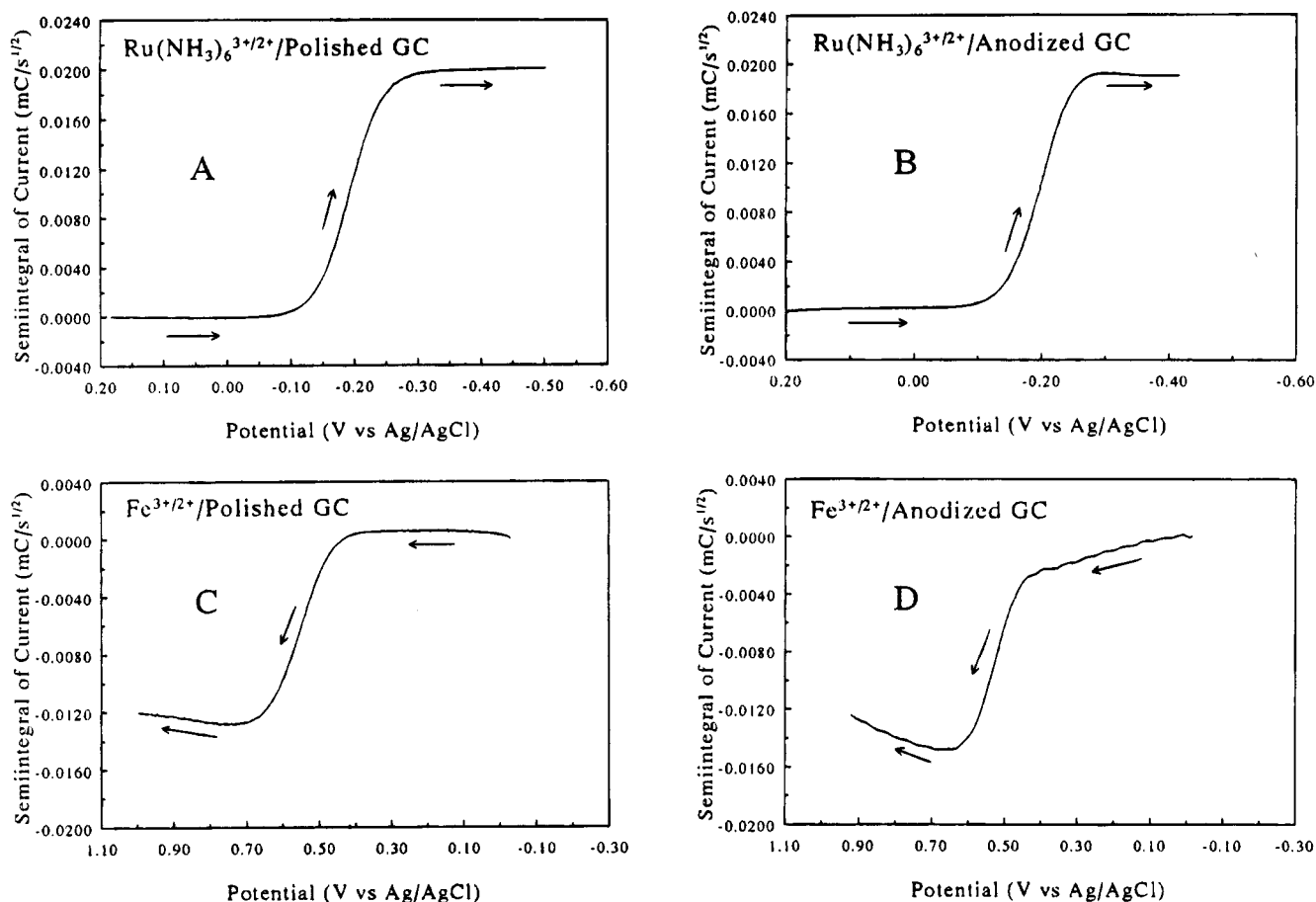


Figure 8. Semiintegrals of (A) 1 mM $\text{Ru}(\text{NH}_3)_6^{3+/2+}$ in 1 M KCl at polished GC electrode ($\nu = 20$ V/s); (B) 1 mM $\text{Ru}(\text{NH}_3)_6^{3+/2+}$ in 1 M KCl at GC electrode after ECP (ECP procedure: three cycles from 0 to 2.2 V in 1 M H_2SO_4 at 0.2 V/s); (C) 1 mM $\text{Fe}^{3+/2+}$ in 0.2 M HClO_4 at polished GC electrode ($\nu = 2$ V/s); and (D) 1 mM $\text{Fe}^{3+/2+}$ in 0.2 M HClO_4 at GC electrode after ECP ($\nu = 0.5$ V/s).

Although the results strongly support the involvement of surface carbonyl groups in electrocatalysis of the aquated systems examined, there remain several possibilities for the mechanism of carbonyl catalysis. Redox mediation by C=O-containing surface groups is unlikely, given the redox potentials of the systems studied. Mediation by a surface group should yield voltammetric waves near the redox potential of the mediator. On the contrary, the $E_{1/2}$ values for $\text{Fe}_{\text{aq}}^{2+/3+}$, $\text{Eu}_{\text{aq}}^{2+/3+}$, and $\text{V}_{\text{aq}}^{2+/3+}$ occur near their expected values, not those of a mediator. A mechanism involving inner-sphere catalysis by adjacent C=O and OH groups proposed earlier is another possibility. The catalysis of $\text{Fe}_{\text{aq}}^{2+/3+}$ by chemisorbed Cl^- on Au noted by Nagy et al. provides a possibly useful analogy.³² In that case, it was concluded that chemisorbed Cl^- provided a bridging group for inner-sphere catalysis, leading to large rate enhancement. For carbon electrodes, a C=O group could be a bridging ligand which is completely blocked by DNPH derivatization. We proposed previously that the carbonyl group could participate with a surface OH group to form a coordination site similar to that of acetoacetone. However, the greater structural information available from the Raman results, combined with the small effect of surface OH derivatization, does not support OH involvement in catalysis. So, if an inner-sphere route is involved, it would require displacement of an H_2O ligand on the redox center by the surface C=O group. A precedent exists for such a mechanism, for $\text{Cr}^{2+/3+}$ binding to amide and ester C=O groups.³³

A third possibility for surface C=O catalysis of aquated ions is "outer-sphere bridging", in which the inner coordination sphere of the redox center is not displaced during electron transfer.³⁴ The catalyst acts as a bridge between two reactants, leading to a transition state involving two redox centers and the bridge. Examples include K^+ catalysis of $\text{Fe}(\text{CN})_6^{3-/4-}$ self-exchange and anion catalysis of Fe^{2+} , Cr^{2+} , and V^{2+} reduction of $\text{Co}(\text{en})_3^{3+}$ and $\text{Co}(\text{phen})_3^{3+}$. By analogy to this mechanism, the $\text{M}_{\text{aq}}^{2+/3+}$ ion would retain its hydration sphere, but the ion would interact with a surface C=O group to promote electron transfer. It is speculation at this point, but such an interaction could involve hydrogen bonding between a complexed water molecule and a surface C=O group. The observation of adsorption of $\text{Fe}_{\text{aq}}^{2+}$ on GC implies that such an interaction may be quite strong.

In summary, $\text{Ru}(\text{NH}_3)_6^{2+/3+}$ and $\text{IrCl}_6^{3-/4-}$ are examples of outer-sphere electron transfer reactions on carbon surfaces. The rates for these systems are insensitive to surface chemistry on disordered carbon electrodes such as glassy carbon, and the observed rates do not vary greatly with surface oxide coverage or the presence of monolayers of nonspecific adsorbers. In contrast, $\text{Fe}_{\text{aq}}^{2+/3+}$, $\text{Eu}_{\text{aq}}^{2+/3+}$, and $\text{V}_{\text{aq}}^{2+/3+}$ are very sensitive to the density of surface C=O groups, which provide a catalytic route to increase an inherently slow outer-sphere rate. Although the structural details of the catalytic mechanism are not yet known,

(33) Cannon, R. D. *Electron Transfer Reactions*; Butterworths: Boston, 1980; pp 156–161.

(34) Reference 33, p 166 ff.

rate enhancement depends on specific interactions with surface carbonyl groups. The strong effect of this specific interaction underlies the extreme sensitivity of $\text{Fe}_{\text{aq}}^{2+/3+}$, $\text{Eu}_{\text{aq}}^{2+/3+}$, and $\text{V}_{\text{aq}}^{2+/3+}$ electron transfer kinetics to surface chemistry on carbon electrodes.

ACKNOWLEDGMENT

This work was supported by the Surface and Analytical Chemistry Division of the National Science Foundation.

Received for review April 3, 1995. Accepted June 29, 1995.*

AC950325B

* Abstract published in *Advance ACS Abstracts*, August 1, 1995.